Comput. Methods Appl. Mech. Engrg. 259 (2013) 1–9

Contents lists available at SciVerse ScienceDirect

Comput. Methods Appl. Mech. Engrg.

journal homepage: www.elsevier.com/locate/cma

A stochastic algorithm for modeling heat welded random carbon nanotube network

M. Kirca [a], X. Yang [b], A.C. To [a,*]

[a] Department of Mechanical Engineering and Materials Science, University of Pittsburgh, PA 15261, USA
[b] Department of Power Engineering, North China Electric Power University, Baoding 071003, China

ARTICLE INFO

Article history:
Received 8 January 2012
Received in revised form 22 January 2013
Accepted 24 February 2013
Available online 13 March 2013

Keywords:
Carbon nanotubes
Network
Foam
Welding

ABSTRACT

Carbon nanotubes (CNTs) are one of the presents of nanotechnology being investigated due to their extraordinary mechanical, thermal and electrical properties. Carbon nanotube networks feed the idea that CNTs can be used as the building blocks of new advanced materials utilizing the superior characteristics of CNTs. In this way, nanoscale features of CNTs can be scaled up to even continuum proportions. In this study, 2-D and 3-D CNT network generation methods are introduced by which the geometrical parameters, such as CNT length, chirality, intersection angle and junctional density, can be controlled and a random CNT network is obtained. Then, molecular dynamics (MD) simulations are used to create covalent bonds between intersecting CNTs, which allow the investigation of the mechanical, thermal and electrical properties of random CNT networks.

1. Introduction

Carbon nanotubes (CNTs) are one of the extraordinary nanomaterials that are promising candidates for thermal, electrical and structural applications due to their unique properties [1,2]. Since their discovery by Iijima (1991), thousands of studies, so far, have been adopted to their exceptional high strength and unusual electrical and thermal properties, displaying the desirable nature of their multifunctional capability. In the last years, the usefulness of CNTs has been enormously extended by their use as CNT networks through which CNTs are self-intersected in two or three dimensional space [3–9]. Because of their strong electrical conductivity with high light transmittance, CNT networks are attractive alternatives to silicon based macroelectronic devices [10]. Initial studies on 2-D CNT networks deposited onto flexible and polymeric substrates have focused on their electronic and sensor properties [11–14]. Several CNT network based thin films have been proposed to obtain lightweight, unbreakable displays and other flexible electronic devices [15]. Bottom-up controlled production of such networks can also enable them to be used in applications such as sensors, filters, composites and electromechanical actuators [1]. However, CNT networks also display the charming mechanical abilities of individual CNTs to macro-mechanical applications such as nanocomposites, similar to CNTs that are used as reinforcing units in nanocomposites, CNT networks can also be employed in nanocomposites for both reinforcement and damage detection purposes [16–18]. In this study, a self-controlled algorithm for generating a 2- or 3-D CNT network consisting of randomly oriented and intersected CNTs has been introduced, and a heat welding method is applied on sample networks to obtain covalently bonded networks by molecular dynamics (MD) simulations.

Furthermore, a recently developed CNT aerogel [4] material that is nanostructured by self-intersecting CNTs forming a random network at the continuum scale is one of the important examples displaying an ultra-high stiffness-to-weight ratio material with conductive properties. Instead of having a reinforcement role in nanocomposites, this material enables the CNT network to constitute a bulk material on its own.

Unquestionably, the electrical, thermal or mechanical properties of CNT networks depend on the density of junctions between CNTs as well as junction properties and impurities throughout the network. It has been shown that electrical conductance and mechanical strength of the junctions may be enhanced by manipulating junction area, i.e. increasing the crossing area [19]. In this manner, the algorithm proposed in this study will provide complete control on the junction properties and all the other geometrical features (e.g. CNT length, diameter, CNT intersection angle), which will enable the exploration of CNT networks theoretically or numerically by using much more realistic models.

Generally, CNT networks can be formed randomly by depositing CNTs locally on the catalyzed substrates by chemical vapor deposition methods (CVD) or depositing from CNT embedded polymeric suspensions remotely by using spin coating, spray coating, or

* Corresponding author. Address: Department of Mechanical Engineering and Materials Science, University of Pittsburgh, 508 Benedum Hall, Pittsburgh, PA 15261, USA. Tel.: +1 (412) 624 2052; fax: +1 (412) 624 4846.
E-mail address: albertto@pitt.edu (A.C. To).

0045-7825/$ - see front matter © 2013 Elsevier B.V. All rights reserved.
http://dx.doi.org/10.1016/j.cma.2013.02.014

vacuum filtration techniques [20–23]. With deposition on the catalyzed substrates, alignment of long CNTs can be more evenly created with directional control, but growth temperatures are high and unwanted byproducts may also be accumulated [23]. Therefore, deposition from solutions with suspended CNTs is much more popular due to the ability to produce them at ambient conditions, despite the time-consuming steps such as purification and dispersion of CNTs.

Most studies investigating the properties of CNT networks are carried out experimentally following a corresponding production phase. For instance, the thermal stability of CNT networks produced by the dielectrophoresis method on microelectrodes has been studied experimentally to predict their uses in electrical applications [24]. Similarly, Wang et al. [19] investigated the electrical and mechanical properties of CNT networks with measurements taken in situ inside the transmission electron microscope. In another experimental study, CNT networks are used as reinforcing materials in composites and compared with composites reinforced by dispersed CNTs [16]. Thostenson and Chou studied the damage and strain sensing capabilities of CNT networks utilized in glass fiber–epoxy composites and have shown through tensile testing that conductive percolating CNT networks can detect the initiation and progression of damage [18]. Several other studies [25–29] exist in literature on the electrical, thermal or mechanical properties of CNT networks carrying out experimental investigations which, as the other aforementioned studies, inherently require equipment of manufacturing and testing. On the other hand, the majority of computational studies have focused on the investigation of individual CNTs and their nanocomposites [30–33]. Due to the lack of a proper method for the generation of random CNT networks and computational limitations, there is a limited number of studies that use numerical models and computational methods for the investigations of CNT networks. Moreover, existing studies [34–39] that employ numerical network models mostly use ordered networks which do not include the geometrical irregularities and other possible imperfections, such as bond rearrangements, at junctions. Moreover, in these models only one type of junctions are modeled. A recently published study [40] investigates the mechanical behavior of short single-walled CNT (SWCNT) aggregates composed of randomly dispersed non-intersected CNTs by molecular mechanics.

In this study, a quasi-random self-intersected CNT network generation algorithm that enables the control of behavior decisive parameters, such as CNT length scale, density of junctions and relative angular position, is presented and several example networks with different parameters mentioned above are generated. Following the generation of a CNT network in which the CNT units are so close together that heating to certain temperatures can yield a covalently bonded network, MD simulations are carried out to obtain bonded networks. As a result, parameter-controlled covalently bonded CNT network models can be further used within MD simulations to investigate mechanical, thermal and electrical properties of CNT networks and their co-operating systems (i.e. nanocomposites).

2. General concepts

The process of generating random networks can be introduced as a process of configuring the network items (in this case, randomly intersected CNTs) randomly in the design space. The placing of network items is carried out under constraints in a random nature. The algorithm explained here is also employed for the generation of random porous networks with spherical cells which is used to model microcellular carbon foams [41].

Before explaining the process of the algorithm, some important concepts that will often be used in the explanation should be defined. First of those, the **design space** is the volume where CNT items are placed randomly. In 2-D network applications, it is defined as a plane with a thickness that encapsulates the CNT units normal to the plane. The other definition, **library**, is just a conceptual library comprised of all the different types of items (CNTs) that will be placed into the design space. Regarding this definition, CNT units used in the random network can differ in length and chirality (diameter). As a result, distinct CNT items can be reserved in the library and chosen randomly before the placement. Another concept, **target**, which is important when putting the selected item into the design space is the item (CNT) on which other items are closely placed to create an interconnected network. Each target element has a number of **cross-linked CNTs** which will be welded on the target element. Finally, CNT items selected from the library can be placed into the design space only if they satisfy certain **design constraints** imposed on the welded network generation. Without satisfying the constraints, the CNT item remains as a **candidate** for the network and it is called a candidate CNT.

3. General algorithm

Network generation is a typical cyclic procedure. At each step of the loop, a new CNT item that satisfies the constraints is placed into the design space. At each step, a number of candidate CNTs are created consecutively and tested against the design constraints until a suitable candidate is found. There are 2 loops in this procedure. The first loop is for continuation of the generation of the CNT items while the second loop is the sub-loop for generation and validation of candidate CNTs. When one of the CNT candidates satisfies all the design constraints in the sub-loop, the generation process continues with the selection of CNT from the library in the main loop. The main procedure can be summarized in 5 steps.

(1) Taking from the library: a candidate CNT item is chosen randomly from the CNT library where multiple CNTs having different lengths and chiralities are stored. For each chirality, the diameters of corresponding CNTs are calculated.
(2) Rotation and translation: After randomly selecting CNTs from the library, they are randomly rotated and translated in the design space.
(3) Checking constraints: After rotation and translation, the design constraints are checked on the candidate CNT.
(4) Making a decision: If the constrains are satisfied, the candidate CNT is placed into the design space. Otherwise, the procedure is restarted from the beginning.
(5) Writing LAMMPS input data file: Atomic coordinates of each CNT item are written into different files instead of storing them in the memory. Using these files (atomic coordinates), the LAMMPS input data file is written to another file.

3.1. Line segment representation of CNTs

To save computational time, CNTs are represented by 3-D line segments passing through the central points of the CNTs cylindrical geometry as shown in Fig. 1.

Each line segment is represented by the coordinates of end points, which are the central points of the circles at the CNTs end. During the generation process, end point coordinates are also stored and written to a file. Rotation and translation operations are also applied to end points, while all distance and angle calculations are done via the line segments instead of atomic coordinates.

The random points on the line segments are generated via parametric line equations as shown in Eq. (1) where $\{x_0, y_0, z_0\}$ and $\{x_1, y_1, z_1\}$ are the tip coordinates and t is the parameter

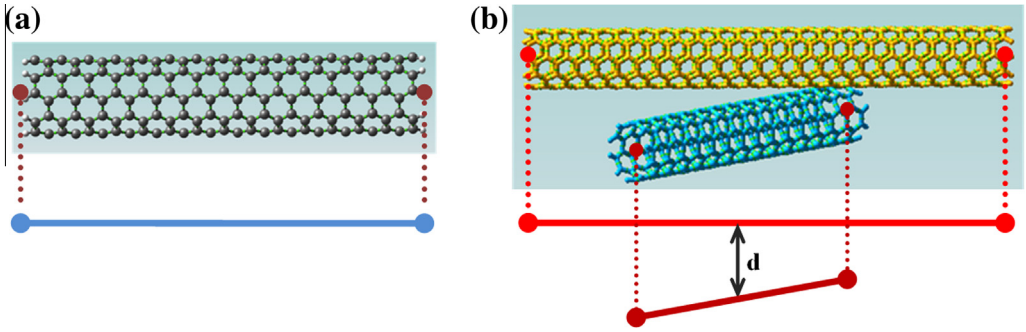

Fig. 1. (a) Line segment representation of CNT and (b) minimum distance between CNTs.

varying in range [0,1] that describes the line segment between the tip coordinates.

$$\begin{aligned} x &= x_0 + t(x_1 - x_0) \\ y &= y_0 + t(y_1 - y_0) \\ z &= z_0 + t(z_1 - z_0) \end{aligned} \tag{1}$$

The line segment parameter t is also used for the further segmentation of line segments to position the candidate CNTs on the target CNT more evenly as represented in Fig. 3. For instance, a constraint of n cross-links on each target CNT is maintained by dividing the interval of t by n. Thus, the kth cross-link is positioned on the target in the interval of $[(k-1)/n, k/n]$.

3.2. Target based approach

After putting the first CNT into the design space, it is assigned as the target on which a certain number of other CNTs should be placed so as to create an interconnected network. As a result, the CNT item that is assigned as the target will host cross-linked CNTs. All subsequent CNTs created after the target assignment should be cross-linked with the target until the number of cross-links reaches the maximum value, which is predefined as a parameter. After the placement of all cross-linked CNTs for a specific target is completed, a new target is assigned and new cross-links are created for this new target.

The target based approach explained above is the philosophy behind the translation operation. Instead of throwing the CNTs into the design space randomly, the translated CNTs are placed in the region close to the target using a systematic method. After rotating the candidate CNT in the library, a guide point (A) is determined randomly on its representative line using parametric functions of that line segment (Eq. (1)) as shown in Fig. 2. Similarly, another guide point (B) is determined on the target line randomly. After determining points A and B, translation is done in the direction of the ***B–A*** vector. In Fig. 2, only the 2-D representation has been shown. For a 2-D network, since the CNTs are rotated in the same plane, i.e. xy plane, translation in the direction of B–A vector results in overlapping of atoms in the intersection region. In order to avoid overlapping, an additional translation (in z direction) is required to keep the CNTs away from each other in a controlled way. For a 3-D network, it is not necessary to do the additional translation in a specific direction.

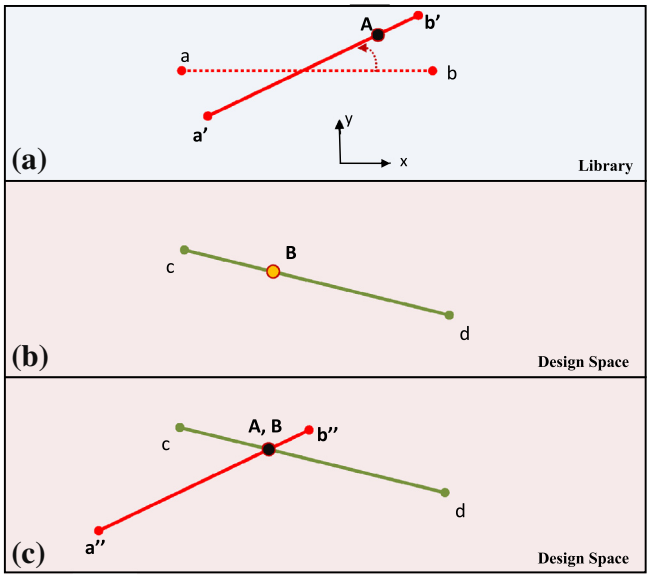

Fig. 2. Process of placing CNT candidates into the design space: (a) rotation of the candidate CNT in library, (b) target CNT in the design space waiting for intersecting CNT coming from library and (c) design space after translation.

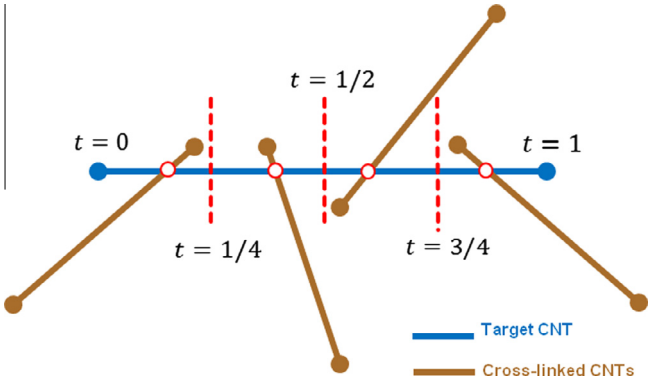

Fig. 3. Segmentations of line segments by dividing the segment domain by the number of cross-links which is 4 in this example.

Using this approach, the probability of a candidate CNT being accepted is much higher. Thus, the number of candidates generated for the new cross-link in the sub-loop is decreased and so the time consumed is highly decreased.

3.3. Checking constraints

There are certain constraints for generated candidate CNTs. If the candidate CNT satisfies these constraints, it is accepted as the cross-linked CNT of the target and its atomic coordinates are written to a separate file named with its identification number. The constraints for candidate CNTs are listed below:

(1) The candidate CNT should be within a specified range of distance to the target so as to be a cross-linked CNT. It should not be closer than a specified distance to the target, and to the other CNTs created before, in order to maintain a stable welded spot between the target and the cross-linked CNTs. Controllability of the alignment of CNTs during the

manufacturing phase by changing the electrical field applied to CNTs [42] highlights the importance of managing the alignments of CNTs in the numerical network model. For this reason, the angle between the candidate CNT and the target CNT, which determines the junction type between two intersecting CNTs, is randomly selected in a predefined range. Line segment representation of the CNTs, as previously explained, are employed to realize the distance and angle constraints for a more controlled network topologies. Mechanical and electrical behavior of different junction types is different as reported in [43–46]. Thus, controlling the type of junctions throughout the network is vital to capture the main characteristic of the network.

(2) A specific distance range between the intersection points can also be predefined and set as a constraint. This distance between the cross-links on the same CNT item is an important parameter to determine the flexibility of the CNT segments between cross-links similar to cross-linked polymer networks [47–49]. For this constraint, line segment parameter t is used to control the position of cross-linked CNTs on the target CNT so that cross-linked CNTs can be evenly distributed on the target as shown in Fig. 3.

Along with these constraints, another constraint can be defined such that the number of the cross-links interconnected with the target CNT should not be less than the specified value. This constraint can be relaxed during the generation process. Due to geometrical difficulties and/or other constraints, sometimes it may be impossible to place a cross-linked candidate CNT around the target. For this circumstance, this constraint is relaxed only for the corresponding target to expedite the generation process. After placing the required number of candidate CNTs on the current target, a new target CNT is selected among the existing CNTs already generated until the number of CNTs in the design space exceeds the predetermined value.

All the constraints which will affect the topology of the network can be arranged in the future according to the detailed characterization results of CNT network materials. Therefore, the proposed method allows experimental characterization data to be employed in computer simulations of the materials behavior. Alternatively, the constraints can be set independently to investigate the effects of several topological parameters such as CNT lengths between two intersection points, the frequency of intersections through the network or the angularity of the intersecting CNTs.

3.4. Making decision

If one of the constraints explained in the previous section is not satisfied, another candidate CNT is selected from the library, rotated, and translated within the design space before being checked against the constraints. This sub-loop is kept active until a suitable candidate satisfying the constraints is found, while the main loop is active until the specified number of CNTs in the design space has been created.

4. Sample networks and welding procedure

In this section, some examples of 2-D and 3-D CNT network models generated by stochastic target based algorithm explained elaborately in the previous sections are presented. In the network models ultra thin CNTs with (5,0) chirality are employed to ensure the junction formation following the annealing process. In Fig. 4,

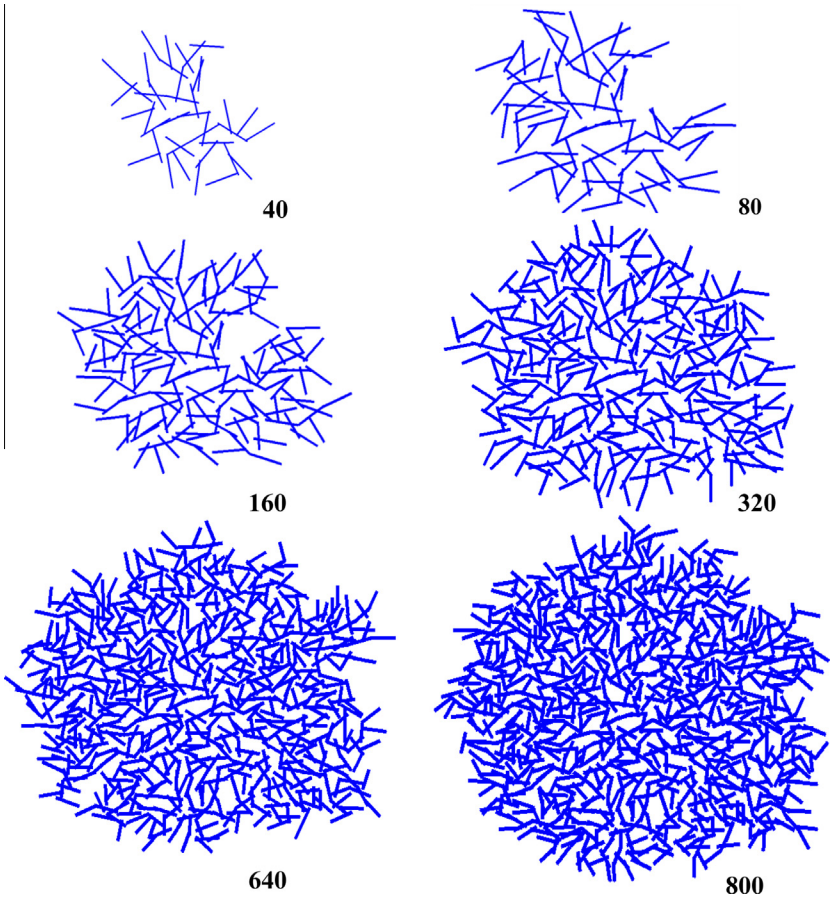

Fig. 4. 2-D network samples with increasing number of CNT units.

network generation process is shown by increasing the number of CNT units in the design space. The network properties can also be changed by modifying the parameters such as the minimum number of junctions per target CNT, minimum distance between cross-linked CNTs and the length of the CNT units. Consequently, this controllability of tuning enables to generate CNT networks in different natures. As can be seen in the Figs. 5–8, several types of junctions (X, Y or T) that play important role on the behavior of CNT networks [43–46] can be observed within the networks randomly. Intersected CNT units are separated before the welding with a wall-to-wall distance (about 4 Å) to avoid van der Waals interaction so that unstable junctions at higher temperatures can be prevented [46,50].

MD simulations in this study are carried out with the LAMMPS code [51]. Interaction between the carbon atoms is modeled by using the Adaptive Intermolecular Reactive Empirical Bond Order (AI-REBO) interatomic potential [52] due to the fact that it allows breaking and formation of covalent bonds. The thermal equilibrium of the system is maintained by Nose–Hoover thermostat and canonical ensemble (NVT) is assigned to the system as thermodynamic characteristic. In order to encourage junction formation at lower temperatures than the referenced temperature values (2500–3500 K) for heat welding procedure [37], small ratio of atoms in the spherical volume centered at the intersecting points is removed to create dangling bonds and the system is relaxed at 300–600 K. Initially, thermostating is applied to only these spherical welding spots, and then the network is relaxed at room temperature. By this way, stability of bonds formed at junction regions is examined. In literature [46], it is reported that without introducing any imperfections such as vacancies or interstitials, covalent bonds can still be generated but in longer computational time.

Initially straight and non inter-bonded CNTs (Fig. 5) become curved with the effect of thermal vibrations and stable covalent bonds are formed (Fig. 6).

The method proposed can also be applicable to continuum scale analysis. Employing the line segment representation of CNTs in the method, the generated network model can be easily converted to a CAD surface or line models, which will enable researchers to carry out finite element (FE) simulations. In this regard, equivalent shell or beam models [53–56] for representing the CNT items can be employed to perform continuum scale analyses. In this way, the time and length scale limitations of classical molecular dynamics simulations can be overcome. As shown in Fig. 9(b), CAD cylindrical surface data can be obtained from the line segments of CNTs and this surface data can be employed to create FE model of the CNT network. The welding at the intersection region can be modeled by beam elements having suitable stiffness values which can be found in literature [56].

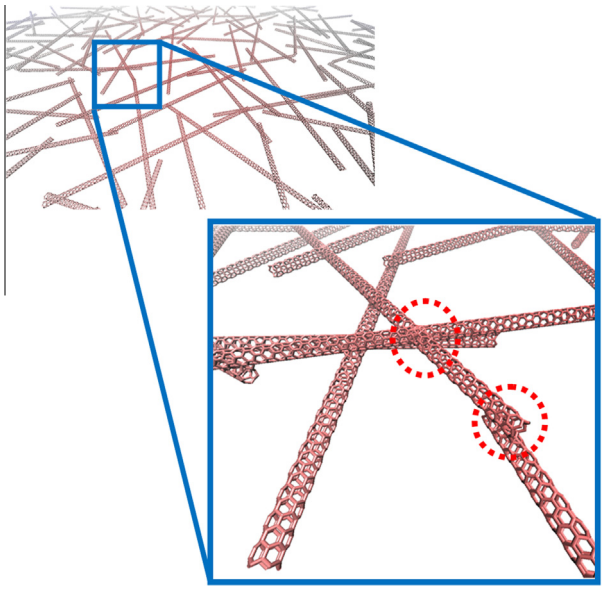

Fig. 5. 2-D network sample showing different junction types and spot areas.

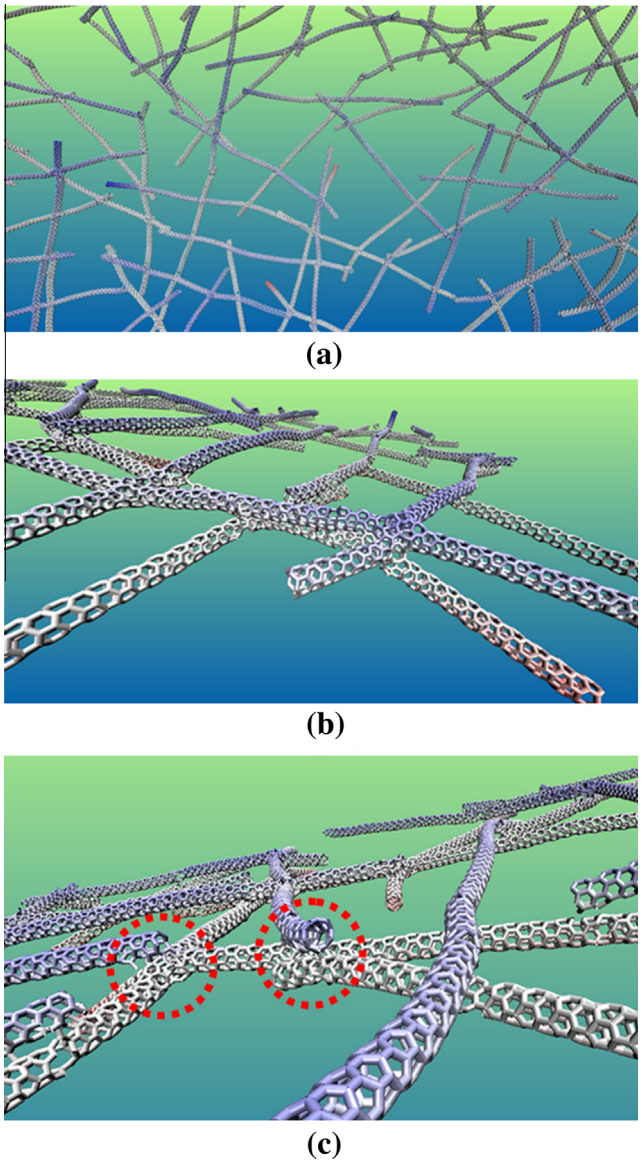

Fig. 6. (a) Top view of a welded 2-D network, (b)–(c) junctions formed after annealing.

4.1. Statistical characterization of random networks

In order to verify the effectiveness of the proposed stochastic generation method, we generate 100 2-D CNT networks and check the morphological parameters controlled in the method against the relevant statistics collected from the networks generated. These parameters include the cross link density, angular orientation of cross-linked CNTs, and distance between two

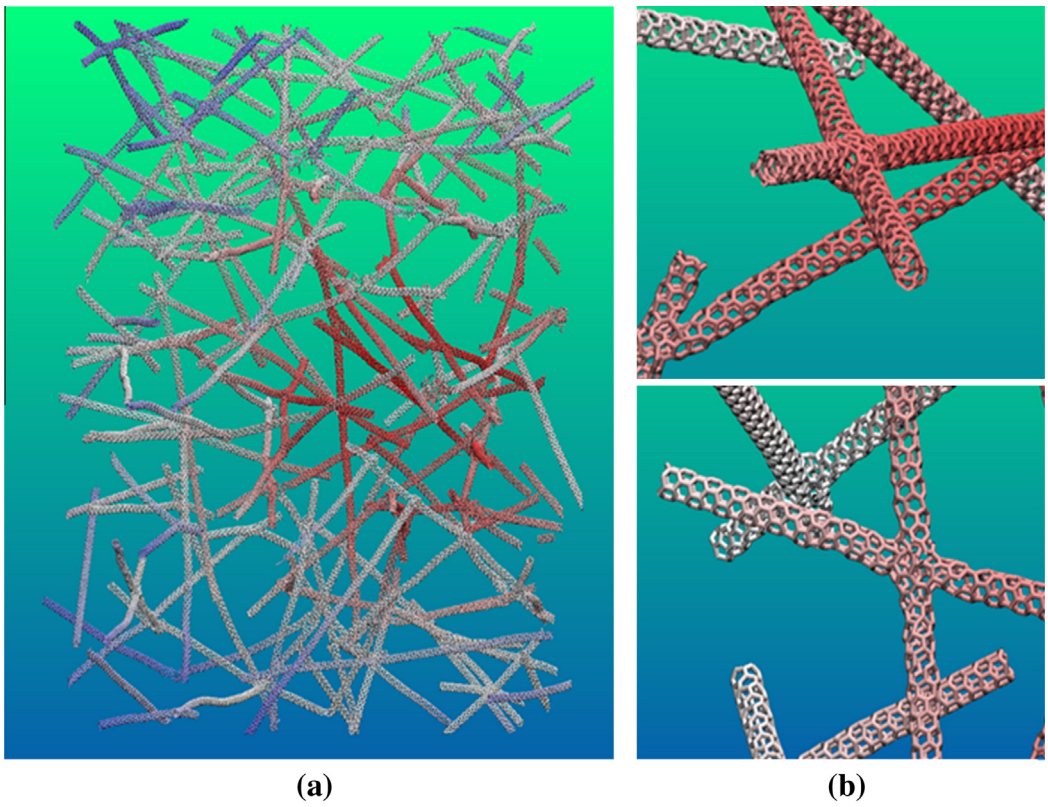

Fig. 7. (a)Perspective view of a 3-D CNT network and (b) snapshots of junctions.

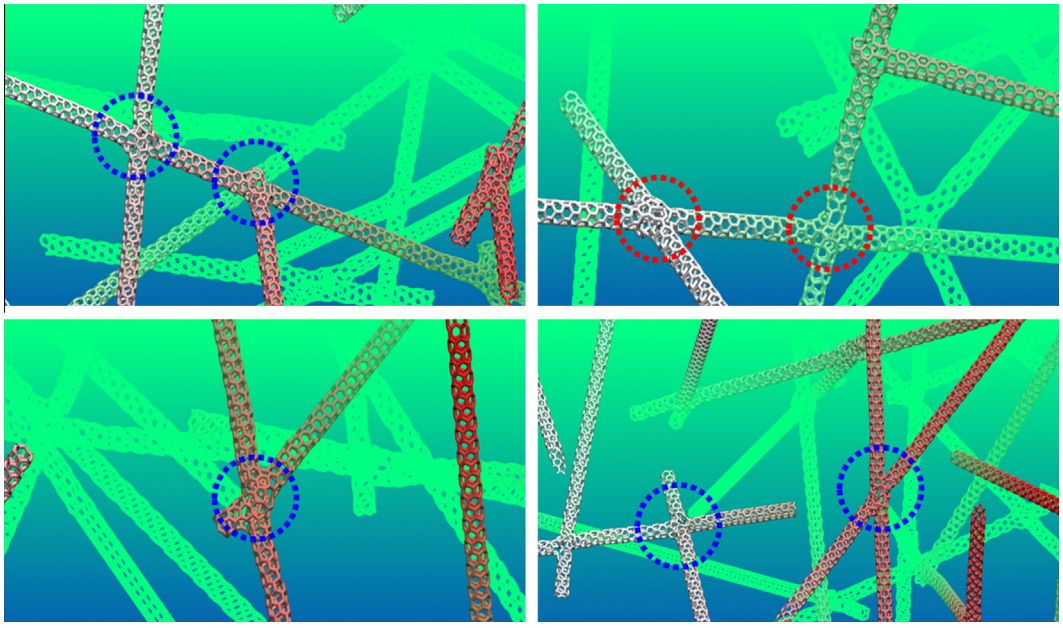

Fig. 8. Example of junctions throughout 3-D CNT network.

adjacent cross-links. In the verification process, 100 2-D network samples consisted of 100 CNTs of 20 nm in length are realized and statistically characterized.

Cross-link density, as explained in Section 3.3, is controlled by the parameter that specifies the expected number of CNTs cross-linked with a target CNT. For the generated network samples this

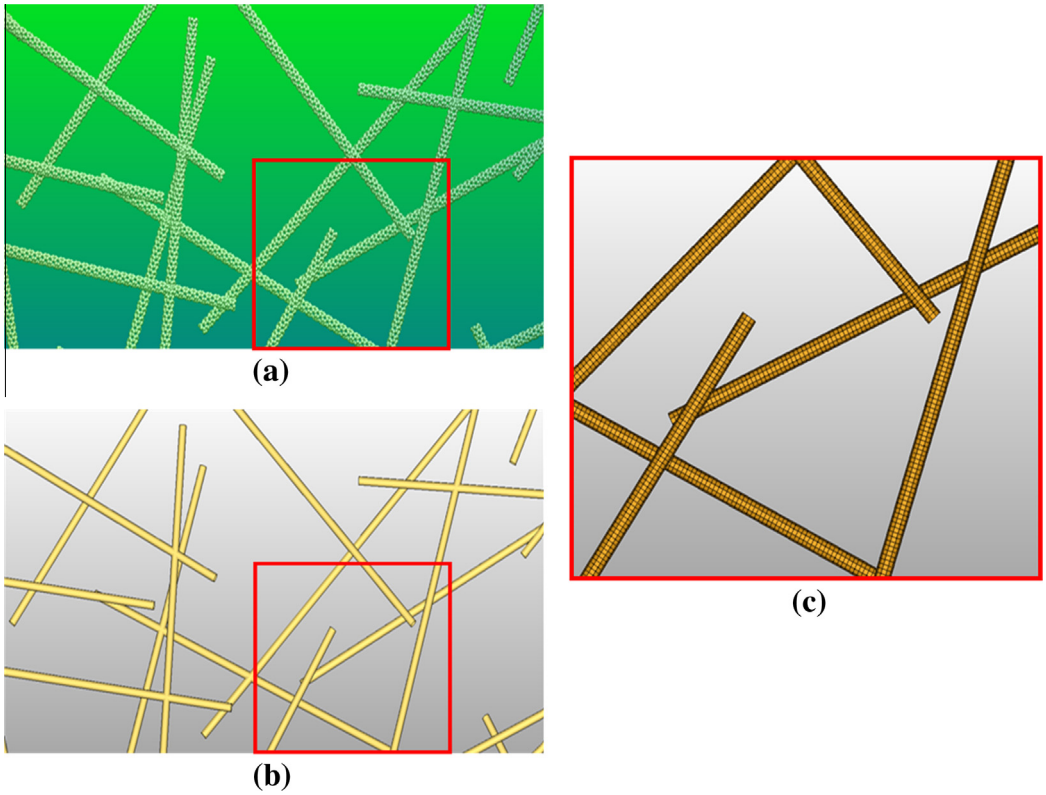

Fig. 9. (a) Atomistic view of 2-D network, (b) surface CAD drawing view of atomistic model and (c) equivalent FE model of the atomistic model.

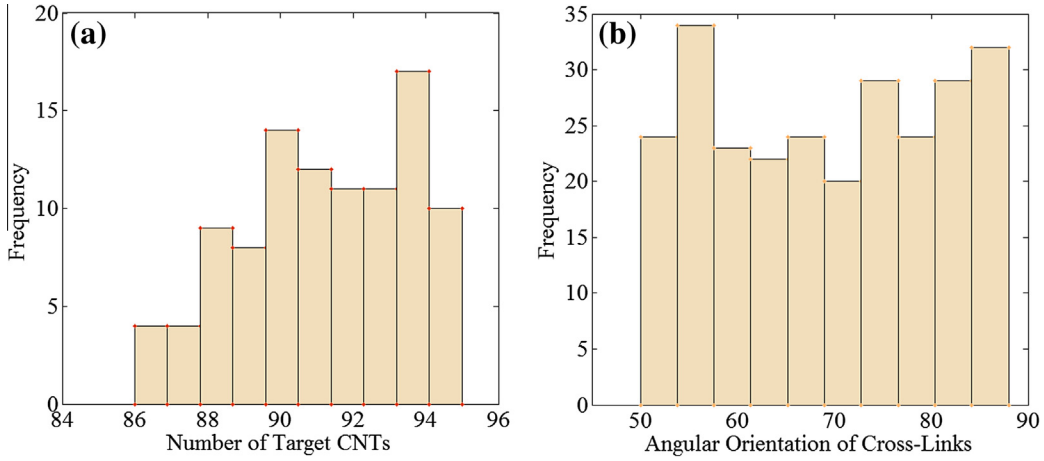

Fig. 10. (a) Distribution of number of target CNTs which are completely cross-linked by 4 CNTs for 100 samples and (b) distribution of acute angles (in degree) between cross-linked CNTs in a single sample of network.

parameter is chosen to be 4 for the 20 nm long CNTs. In Fig. 10(a), for the 100 networks generated, the distribution of the number of target CNTs that are cross-linked by 4 other CNTs in each network is presented. As mentioned before, when geometrical impossibility emerges during the CNT generation process, the controlled parameter of 4 cross-links per target CNT is relaxed in order to continue to the subsequent steps in the network generation. Therefore, the maximum number of CNTs that have 4 cross-links will be less than total number of CNTs (i.e. 100 in this case). In the current characterization, the minimum and maximum number of fully covered CNTs are determined to be 86 and 95, respectively, for the 100 CNTs as shown in Fig. 10(a). Based on these results, with the proposed stochastic method, it has been shown that the cross-link density defined as a design parameter can be maintained fairly well in the generated networks.

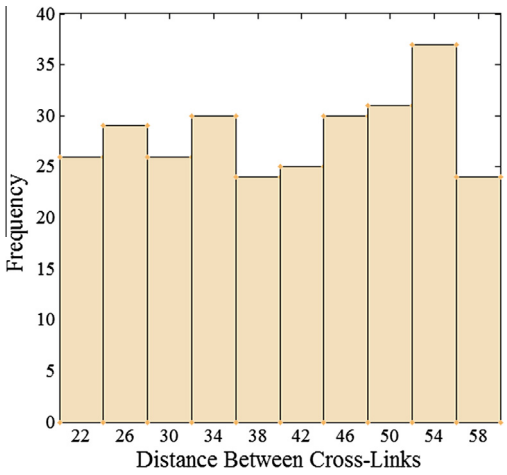

Fig. 11. Distribution of distances between cross-links on the same CNT for one of the sample network.

For the CNT networks generated, another parameter that is being controlled is the angular orientation of cross-linked CNTs relative to each other. The angular constraint for these samples is applied in two stages. In the first stage, attempts are made to keep the angles between 65° and 75°. In the event of impasse during the CNT generation process, the first stage constraint is relaxed gradually to the second stage constraint predefined as the range of 45–90°. Fig. 10(b) illustrates distribution of the acute angles within a network generated is shown to be within the range of 50–88° quite evenly between cross-linked CNTs, which shows that the angular constraints can be utilized correctly and efficiently. As a consequence, successful application of the angular constraints will yield typical CNT junctions (e.g. X, Y or T).

Additionally, the distance between the adjacent cross-links on the same CNT is maintained to be within a predefined range of 20–60 nm. The distribution of the distance values of adjacent cross-links on the same CNT within a network sample is given in Fig. 11 and shows a pseudo-uniform distribution between 20 and 60 mm. In accordance with this result, all the cross-link distances can be kept within a specified range.

Fig. 12(a) and (b) shows distribution of mean values of cross-link angles and mean values of cross-link distances, respectively, for 100 2-D network samples. While the respective mean values are defined to be 70° and 40 nm, those obtained from the generated networks are 68.9° and 39.8 nm, respectively. As can be observed from the figures, the scatter around the mean values is very small. Therefore, it can be concluded that the objective mean values can be captured with high precision.

The above characterization results have demonstrated the effectiveness of the proposed random network generation method. Hence, networks with tailored morphology can be accurately generated by setting the parameters controlled in the method to the appropriate values.

5. Conclusion

In this study, a stochastic algorithm has been developed to model 2-D and 3-D CNT networks with random geometrical parameters such as CNT orientation and intersection angles. While some parameters are let to be random in nature, some parameters such as CNT chirality and length scale, junctional density, limit angles for intersections can be managed independently. Intersecting regions of CNT networks with proposed method are welded following canonical MD simulations by heating and stable covalent bond formations are obtained. Finally, 2-D or 3-D CNT networks are generated with controllable parameters and can be employed for further mechanical, electrical or thermal studies (Figs. 6 and 7). Due to the controllability efficiency on the topological features of CNT networks and simplicity of the generation algorithm, this CNT network generation method may significantly increase the numerical and theoretical investigations on the CNT networks. The method proposed is also applicable to continuum scale analyses in order to overcome the time and length scale limitations of classical MD simulations. Due to line segment representation of CNTs in the method, the generated network model can be easily converted to a CAD surface or line models, which will enable researchers to carry out FE simulations. Furthermore, following this study, mechanical, thermal or electrical properties of CNT networks can be optimized by changing the topological parameters, and manufacturing techniques can be developed or improved to produce optimized networks.

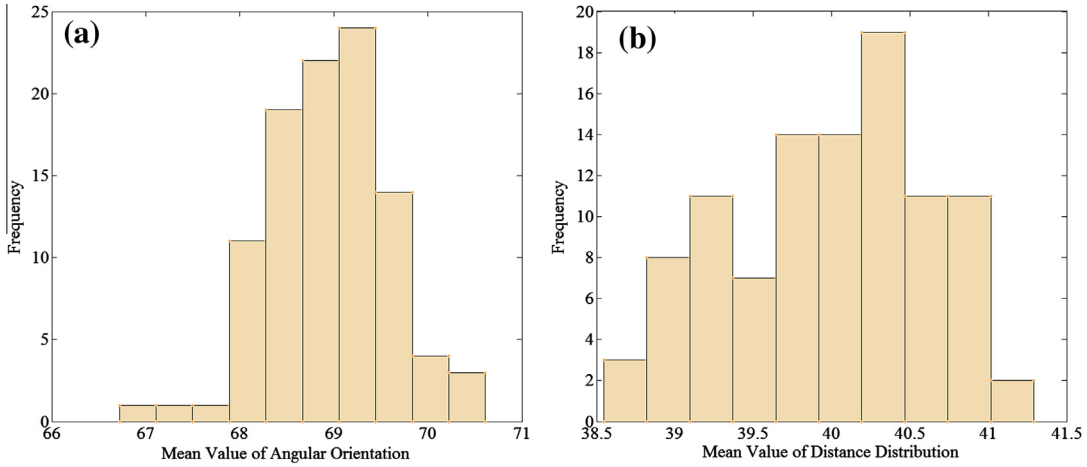

Fig. 12. (a) Distribution of mean values of cross-link angularity through 100 samples and (b) distribution of mean values of cross-link distances through 100 samples.

References

[1] R.H. Baughman, A.A. Zakhidov, W.A. de Heer, Carbon nanotubes – the route towards applications, Science 297 (2002) 787–792.
[2] J. Hu, T.W. Odom, C.M. Lieber, Chemistry and physics in one-dimension: synthesis and properties of nanowires and nanotubes, Acc. Chem. Res. 32 (1999) 435–445.
[3] C.M. Leroy, F. Carn, M. Trinquecoste, R. Backov, P. Delhaes, Multiwalled-carbon-nanotube-based carbon foams, Carbon 45 (2007) 2317–2320.
[4] M.B. Bryning, D.E. Milkie, M.F. Islam, L.A. Hough, J.M. Kikkawa, A.G. Yodh, Carbon nanotube aerogels, Adv. Mater. 19 (2007) 661–664.
[5] M.A. Worsley, S.O. Kucheyev, J.H. Satcher, A.V. Hamza, T.F. Baumann, Mechanically robust and electrically conductice carbon nanotube foams, Appl. Phys. Lett. 94 (2009) 073115.
[6] M. Nabeta, M. Sano, Nanotube foam prepared by gelatin gel as a template, Langmuir 21 (2005) 1706–1708.
[7] S. Kaur, P.M. Ajayan, R.S. Kane, Design and characterization of three-dimensional carbon nanotube foams, J. Phys. Chem. B 110 (2006) 21377–21380.
[8] N. Chakrapani, B. Wei, A. Carrillo, P.M. Ajayan, R.S. Kane, Capillarity-driven assembly of two-dimensional cellular carbon nanotube foams, Natl. Acad. Sci. USA 101 (2004) 4009–4012.
[9] Y. Yang, M.C. Gupta, K.L. Dudley, R.W. Lawrence, Novel carbon nanotube-polystyrene foam composites for electromagnetic interference shielding, Nano Lett. 5 (2005) 2131–2134.
[10] H.S. Lee, C.H. Yun, S.K. Kim, J.H. Choi, C.J. Lee, H.J. Jin, H. Lee, S.J. Park, M. Park, Percolation of two-dimensional multiwall carbon nanotube networks, Appl. Phys. Lett. 95 (2009) 134104.
[11] E.S. Snow, J.P. Novak, P.M. Campbell, D. Park, Random networks of carbon nanotubes as an electronic material, Appl. Phys. Lett. 82 (2003) 2145–2147.
[12] E.S. Snow, J.P. Novak, M.D. Lay, E.H. Houser, F.K. Perkins, P.M. Campbell, Carbon nanotube networks: nanomaterial for macroelectronic applications, J. Vac. Sci. Technol. B 22 (2004) 1990–1994.
[13] L. Jaber- Ansari, M.G. Hahm, T.H. Kim, S. Somu, A. Busnaina, Y.J. Jung, Large scale highly organized single-walled carbon nanotube networks for electrical devices, Appl. Phys. A-Mater. 96 (2009) 373–377.
[14] Y. Tu, Y. Lin, W. Yantasee, Z. Ren, Carbon nanotubes based nanoelectrode arrays: fabrication, evaluation, and application in voltammetric analysis, Electroanalysis 17 (2004) 79–84.
[15] P.J. Novak, M.D. Lay, F.K. Perkins, E.S. Snow, Macroelectronic applications of carbon nanotube networks, Solid State Electron. 48 (2004) 1753–1756.
[16] N.H. Tai, M.K. Yeh, J.H. Liu, Enhancement of the mechanical properties of carbon nanotube/phenolic composites using a carbon nanotube network as the reinforcement, Carbon 42 (2004) 2735–2777.
[17] C. Li, T.W. Chou, Modeling of damage sensing in fiber composites using carbon nanotube networks, Compos. Sci. Technol. 68 (2008) 3373–3379.
[18] E.T. Thostenson, T.W. Chou, Carbon nanotube networks: sensing of distributed strain and damage for life prediction and self healing, Adv. Mater. 18 (2006) 2837–2841.
[19] M. Wang, J. Wang, Q. Chen, L.M. Peng, Fabrication and electrical and mechanical properties of carbon nanotube interconnections, Adv. Funct. Mater. 15 (2005) 1825–1831.
[20] M.Y. Zavodchikova, A.G. Nasibulin, T. Kulmala, K. Grigoras, A.S. Anisimov, S. Franssila, V. Ermolov, E.I. Kauppinen, Novel carbon nanotube network deposition technique for electronic device fabrication, Phys. Stat. Sol. (b) 245 (2009) 2272–2275.
[21] A.M. Cassell, G.C. McCool, H. Tee Ng, J.E. Koehne, B. Chen, J. Li, J. Han, M. Meyyappan, Carbon nanotube networks by chemical vapor deposition, Appl. Phys. Lett. 82 (2003) 817–819.
[22] E.Y. Jang, T.J. Kang, H.W. Im, D.W. Kim, Y.H. Kim, Single-walled carbon-nanotube networks on large area glass substrate by the dip-coating method, Small 12 (2008) 2255–2261.
[23] M.Y. Zavodchikova, T. Kulmala, A.G. Nasibulin, V. Ermolov, S. Franssila, K. Grigoras, E.I. Kauppinen, Carbon nanotube thin film transistors based on aerosel methods, Nanotechnology 20 (2009) 085201.
[24] M. Dimaki, P. Bøggild, W. Svendsen, Temperature response of carbon nanotube networks, J. Phys.: Conf. Ser. 61 (2007) 247–251.
[25] S.S. Rahatekar, K.K. Koziol, S.R. Kline, E.K. Hobbie, J.W. Gilman, A.H. Windle, Length-dependent mechanics of carbon-nanotube networks, Adv. Mater. 21 (2009) 874–878.
[26] G. Gorrasi, R.D. Lieto, G. Patimo, S.D. Pasquale, A. Sorrentino, Structure-property relationships on uniaxially oriented carbon nanotube/polyethylene composites, Polymer 52 (2011) 1124–1132.
[27] L. Chen, R. Ozisik, L.S. Schadler, The influence of carbon nanotube aspect ratio on the foam morphology of MWNT/PMMA nanocomposite foams, Polymer 51 (2010) 2368–2375.
[28] P. Slobodian, P. Riha, A. Lengalova, P. Saha, Compressive stress-electrical conductivity characteristics of multiwall carbon nanotube networks, J. Mater. Sci. 46 (2011) 3186–3190.
[29] L.J. Hall, V.R. Coluci, D.S. Galvao, M.E. Kozlov, M. Zhang, S.O. Dantas, R.H. Baughman, Sign change of Poisson's ratio for carbon nanotube sheets, Science 320 (2008) 504–507.
[30] Y. Jin, F.G. Yuan, Simulation of elastic properties of single-walled carbon nanotubes, Compos. Sci. Technol. 63 (2003) 1507–1515.
[31] C. Li, T.W. Chou, A structural mechanics approach for the analysis of carbon nanotubes, Int. J. Solids Struct. 40 (2003) 2487–2499.
[32] S.J.V. Frankland, V.M. Harik, G.M. Odegard, D.W. Brenner, T.S. Gates, The stress–strain behavior of polymer–nanotube composites from molecular dynamics simulation, Compos. Sci. Technol. 63 (2003) 1655–1661.
[33] T. Belytschko, S.P. Xiao, G.C. Schats, R.S. Ruoff, Atomistic simulations of nanotube fracture, Phys. Rev. B 65 (2002) 2354301–2354308.
[34] Y. Li, X. Qiu, Y. Yin, F. Yang, Q. Fan, The specific heat of carbon nanotube networks and their potential applications, J. Phys. D: Appl. Phys. 42 (2009) 155405.
[35] Y. Lin, W. Cai, X. Shao, Fullerenes connected nanotubes: an approach to build multidimensional carbon nanocomposites, Chem. Phys. 331 (2006) 85–91.
[36] V.R. Coluci, S.O. Dantas, A. Jorio, D.S. Galvao, Mechanical properties of carbon nanotube networks by molecular mechanics and impact molecular dynamics calculations, Phys. Rev. B 75 (2007) 075417.
[37] F.Y. Meng, S.Q. Shi, D.S. Xu, R. Yang, Size effect of X-shaped carbon nanotube junctions, Carbon 44 (2006) 1263–1266.
[38] Y. Li, X. Qiu, F. Yang, Y. Yin, Q. Fan, Stretching-dominated deformation mechanism in a super square carbon nanotube network, Carbon 47 (2009) 812–819.
[39] A.L.M. Reddy, S. Ramaprabhu, Design and fabrication of carbon nanotube-based microfuel cell and fuel cell stack coupled with hydrogen storage device, Int. J. Hydrogen Energ. 32 (2007) 4272–4278.
[40] M. Lan, H. Waisman, Mechanics of SWCNT aggregates studied by incremental constrained minimization, J. Nanomech. Micromech. 2 (2012) 15–22.
[41] M. Kirca, A. Gul, E. Ekinci, F. Yardim, A. Mugan, Computational modeling of micro-cellular carbon foams, Finite Elem. Anal. Des. 44 (2007) 45–52.
[42] Z. Chen, Y. Yang, F. Chen, Q. Qing, Z. Wu, Z. Liu, Controllable interconnection of single-walled carbon nanotubes under AC electric field, J. Phys. Chem. A 109 (2005) 11420–11423.
[43] M. Terrones, F. Banhart, N. Grobert, J.-C. Charlier, H. Terrones, P.M. Ajayan, Molecular junctions by joining single-walled carbon nanotubes, Phys. Rev. Lett. 89–7 (2002) 075505.
[44] L.P. Biro, Z.E. Horvath, G.I. Mark, Z. Osvath, A.A. Koos, A.M. Benito, W. Maser, Ph. Lambin, Carbon nanotube Y junctions: growth and properties, Diam. Relat. Mater. 13 (2004) 241–249.
[45] M. Menon, D. Srivastava, Carbon nanotube "T Junctions": nanoscale metal-semiconductor-metal contact devices, Phys. Rev. Lett. 79–22 (1997) 4453–4456.
[46] F.Y. Meng, S.Q. Shi, D.S. Xu, R. Yang, Multiterminal junctions formed by heating ultrathin single-walled carbon nanotubes, Phys. Rev. B 70 (2004) 125418.
[47] G. Gruner, Two-dimensional carbon nanotube networks: a transparent electronic material, Mater. Res. Soc. Symp. Proc. 905 E (2006). 0905-DD06-05.
[48] N. Fakhri, D.A. Tsyboulski, L. Cognet, R.B. Weisman, M. Pasquali, Diameter-dependent bending dynamics of single-walled carbon nanotubes in liquids, Proc. Natl. Acad. Sci. 106–34 (2009) 14219–14223.
[49] J. Kierfield, K. Baczynski, P. Gutjahr, T. Kuhne, R. Lipowsky, Modelling semiflexible polymers: shape analysis, buckling instabilities, and force generation, Soft Matter 6 (2010) 5764–5769.
[50] N.M. Piper, Y. Fu, J. Tao, X. Yang, A.C. To, Vibration promotes heat welding of single walled nanotubes, Chem. Phys. Lett. 502 (2011) 231–234.
[51] S. Plimpton, Fast parallel algorithms for short-range molecular-dynamics, J. Comput. Phys. 117 (1995) 1–19.
[52] D.W. Brenner, O.A. Shenderova, J.A. Harrison, S.J. Stuart, B. Ni, S.B. Sinnott, A second-generation reactive empirical bond order (REBO) potential energy expression for hydrocarbons, Phys. Rev. B 14 (2002) 783–802.
[53] S. Govindjee, J.L. Sackman, On the use of continuum mechanics to estimate the properties of nanotubes, Solid State Commun. 110 (1999) 227–230.
[54] M. Cinefra, E. Carrera, S. Brischetto, Refined shell models for the vibration analysis of multiwalled carbon nanotubes, Mech. Adv. Mater. Struc. 18–7 (2011) 476–483.
[55] C.Y. Wang, L.C. Zhang, An elastic shell model for characterizing single-walled carbon nanotubes, Nanotechnology 19 (2008) 195704–195710.
[56] K.I. Tserpes, P. Papanikos, Finite element modeling of single-walled carbon nanotubes, Compos. Part B-Eng. 36 (2005) 468–477.